ACS Synthetic Biology
Research Article
Cite This: ACS Synth. Biol. 2019, 8, 2092−2105
pubs.acs.org/synthbio

Developing a Versatile Shotgun Cloning Strategy for Single-Vector-Based Multiplex Expression of Short Interfering RNAs (siRNAs) in Mammalian Cells

Xi Wang,[a,b] Chengfu Yuan,[b,c] Bo Huang,[a,b,‖] Jiaming Fan,[a,b] Yixiao Feng,[b,d] Alexander J. Li,[b] Bo Zhang,[b,e] Yan Lei,[b,d] Zhenyu Ye,[b,f] Ling Zhao,[b,d] Daigui Cao,[b,d,g] Lijuan Yang,[b,e] Di Wu,[b] Xian Chen,[b,h] Bin Liu,[b,i] William Wagstaff,[b] Fang He,[b,d] Xiaoxing Wu,[b,d] Huaxiu Luo,[b,j] Jing Zhang,[b,d] Meng Zhang,[b,k] Rex C. Haydon,[b] Hue H. Luu,[b] Michael J. Lee,[b] Jennifer Moriatis Wolf,[b] Ailong Huang,[l] Tong-Chuan He,*[,b] and Zongyue Zeng*[,a,b,l]

[a]Ministry of Education Key Laboratory of Diagnostic Medicine, and School of Laboratory and Diagnostic Medicine, Chongqing Medical University, Chongqing, 400016, China

[b]Molecular Oncology Laboratory, Department of Orthopaedic Surgery and Rehabilitation Medicine, The University of Chicago Medical Center, Chicago, Illinois 60637, United States

[c]Department of Biochemistry and Molecular Biology, China Three Gorges University School of Medicine, Yichang, 443002, China

[‖]Department of Clinical Laboratory Medicine, the Second Affiliated Hospital of Nanchang University, Nanchang, 330006, China

[d]The Affiliated Hospitals of Chongqing Medical University, Chongqing, 400016, China

[e]Key Laboratory of Orthopaedic Surgery of Gansu Province, and the Departments of Orthopaedic Surgery and Obstetrics and Gynecology, the First and Second Hospitals of Lanzhou University, Lanzhou, 730030, China

[f]Department of General Surgery, the Second Affiliated Hospital of Soochow University, Suzhou, 215004, China

[g]Department of Orthopaedic Surgery, Chongqing General Hospital, Chongqing, 400013, China

[h]Department of Clinical Laboratory Medicine, The Affiliated Hospital of Qingdao University, Qingdao, 266061, China

[i]School of Life Sciences, Southwest University, Chongqing, 400715, China

[j]Department of Burn and Plastic Surgery, West China Hospital of Sichuan University, Chengdu, 610041, China

[k]Department of Orthopaedic Surgery, The First Affiliated Hospital, Guangzhou University of Chinese Medicine, Guangzhou, 510405, China

[l]Key Laboratory of Molecular Biology for Infectious Diseases of The Ministry of Education of China, Institute for Viral Hepatitis, Department of Infectious Diseases, The Second Affiliated Hospital, Chongqing Medical University, Chongqing, China

Supporting Information

ABSTRACT: As an important post-transcriptional regulatory machinery mediated by ∼21nt short-interfering double-stranded RNA (siRNA), RNA interference (RNAi) is a powerful tool to delineate gene functions and develop therapeutics. However, effective RNAi-mediated silencing requires multiple siRNAs for given genes, a time-consuming process to accomplish. Here, we developed a user-friendly system for single-vector-based multiplex siRNA expression by exploiting the unique feature of restriction endonuclease BstXI. Specifically, we engineered a BstXI-based shotgun cloning (BSG) system, which consists of three entry vectors with siRNA expression units (SiEUs) flanked with distinct BstXI sites, and a retroviral destination vector for shotgun SiEU assembly. For proof-of-principle studies, we constructed multiplex siRNA vectors silencing β-catenin and/or Smad4 and assessed their functionalities in mesenchymal stem cells (MSCs). Pooled siRNA cassettes were effectively inserted into respective entry vectors in one-step, and shotgun seamless assembly of pooled BstXI-digested SiEU fragments into a retroviral destination vector followed. We found these multiplex siRNAs effectively silenced β-catenin and/or Smad4, and inhibited Wnt3A- or BMP9-specific reporters and downstream target expression in MSCs. Furthermore, multiplex silencing of β-catenin and/or Smad4 diminished Wnt3A and/or BMP9-induced osteogenic differentiation. Collectively, the BSG system is a user-friendly technology for single-vector-based multiplex siRNA expression to study gene functions and develop experimental therapeutics.

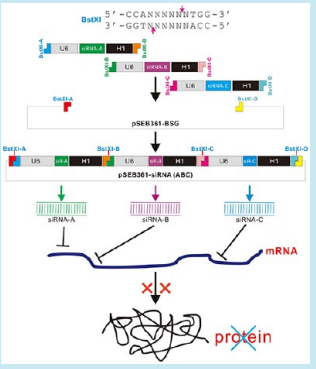

KEYWORDS: *RNA interference (RNAi), short interfering double-stranded RNA (siRNA), Wnt/β-catenin signaling, BMP9/Smad4 signaling, mesenchymal stem cells (MSCs), osteogenic differentiation, multiplex expression, shotgun cloning*

INTRODUCTION

Originally discovered in *C. elegans* as a protecting mechanism against invasion by foreign genes, RNA interference (RNAi) has

Received: May 4, 2019
Published: August 29, 2019

DOI: 10.1021/acssynbio.9b00203
ACS Synth. Biol. 2019, 8, 2092−2105

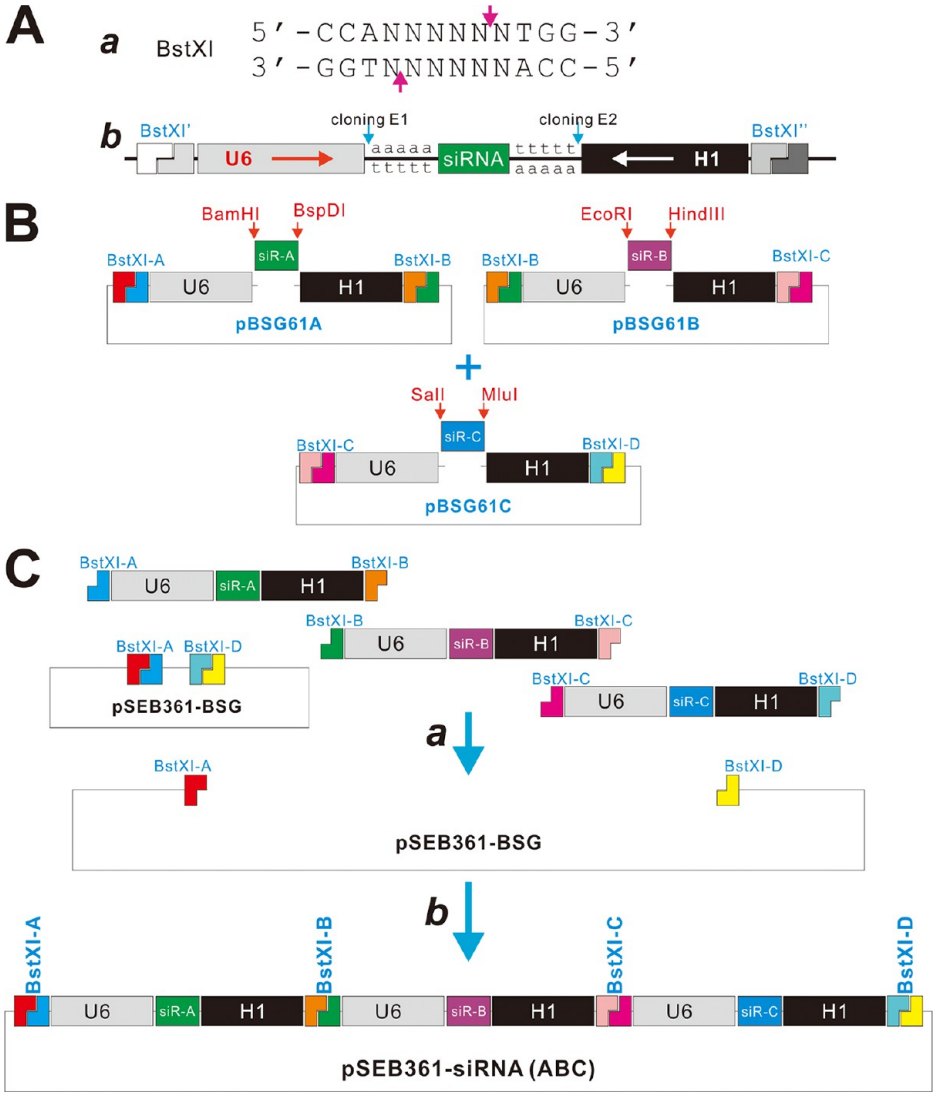

Figure 1. A schematic representation of the BstXI-based shotgun (BSG) cloning strategy for the expression of multiplex (three) siRNAs in a single vector. (A) Schematic depiction of the modular siRNA expression unit (SiEU) flanked by two distinct BstXI sites (a). A prototypic BxtXI recognition site is shown (b), where N represents any nucleotide, and the cleavage sites on both strands are indicated with red arrows. A siRNA oligonucleotide cassette is first cloned into unique restriction sites E1 and E2; and its expression is driven by the converging U6 and H1 promoters. (B) The shotgun cloning of individual siRNA oligo cassettes (SiOCs) at unique restriction sites. The representative three-siRNAs, that is, siR-A, siR-B, and siR-C, are first simultaneously cloned into the unique restriction sites of the entry vectors, pBSG361A, pBSG361B, and pBSG361C (see Supplemental Figure 1A–1C). (C) The one-step assembly of multiple siRNA expression units (SiEUs) through shotgun ligation at distinct BstXI sites, namely BstXI-A through BstXI-D. The three individual SiEUs are first released from pBSG361 entry vectors by BstXI digestion (a), and are simultaneously assembled into a retroviral destination vector, pSEB361-BSG (see Supplemental Figure 1D) at BstXI-A and BstXI-D sites, resulting in the pSEB361-siRNA (ABC) (b), which expresses three different siRNAs.

subsequently been found in diverse eukaryotes.[1−4] The RNAi is a sequence-specific, post-transcriptional silencing process, which is initiated by ∼21nt short interfering double-stranded RNAs (siRNA) homologous to the gene being suppressed and mediated by the RNA-induced silencing complex (RISC).[1−3] Since its discovery about 20 years ago, RNAi has become a powerful tool to study gene functions *in vitro* and *in vivo*.[4] Furthermore, the gene-specific targeting feature of RNAi offers unprecedented opportunities for developing novel therapeutics for human diseases, which is highlighted by the recent US FDA and European Commission's approval of the first RNAi-based drug, ONPATTRO (Patisiran), for the treatment of the polyneuropathy of hereditary transthyretin-mediated (hATTR) amyloidosis in adults in August 2018.[2,3,5−8] Such a milestone event in RNAi therapeutics development, together with the key advances in the design, delivery, and modification technologies of RNAi drugs, is likely to move more candidate RNAi drugs to preclinical and clinical pipelines in coming years.[2,3,5]

Nonetheless, the practical applications of siRNA-based gene silencing require effective expression and delivery of siRNAs into target cells transiently and/or for long-term expression.[7−12] RNAi is usually achieved by delivering chemically synthesized double-stranded siRNA into cells, or by expressing short hairpin RNAs (shRNAs) or siRNAs in cells.[9,11,12] However, RNAi-mediated gene silencing usually necessitates the use of multiple siRNA target sites for a gene of interest, a time-consuming process to construct. We previously developed the pSOS system, in which the siRNA duplexes are made from an oligo cassette driven by converging U6 and H1 promoters.[13] While effective,

DOI: 10.1021/acssynbio.9b00203
ACS Synth. Biol. 2019, 8, 2092−2105

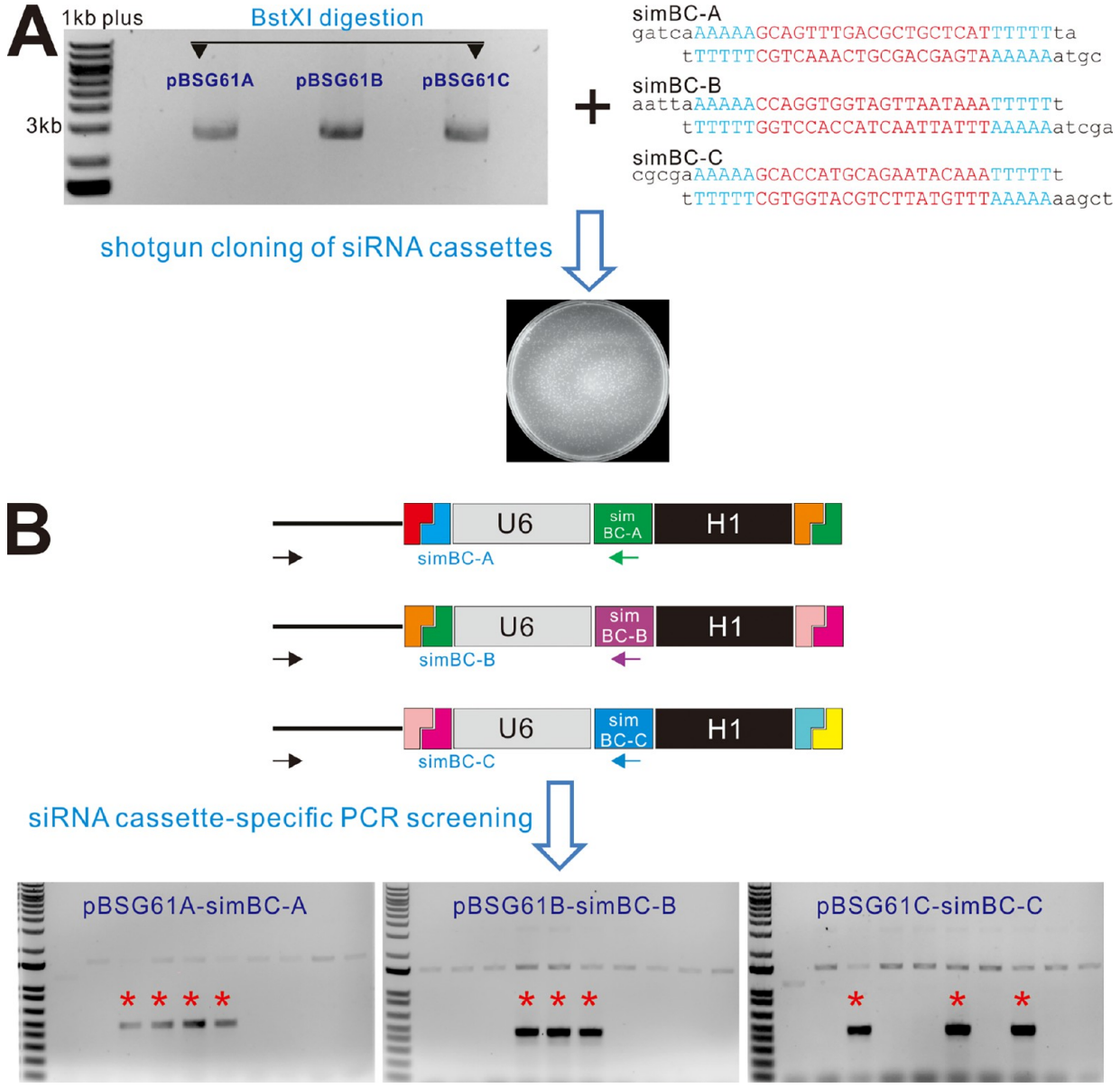

Figure 2. Shotgun cloning of three siRNAs targeting mouse β-catenin (simBC) into the entry vectors. (A) The pBSG361A/B/C entry vectors were digested with BstXI, while the oligonucleotides for the three siRNA target sites of mouse β-catenin were annealed to form double-stranded oligo cassettes. Shotgun ligation was carried out by mixing the three entry vectors with the three simBC oligo cassettes in one ligation reaction. (B) Identification of individual SiEU clones through PCR colony screening with SiEU-specific primers. The PCR screening reactions employed the same upstream primer derived from the pBSG361 entry vectors and the reverse primers of individual SiEUs. PCR screening results from randomly picked 10 clones were shown for each simBC vector. Positive clones are indicated with red asterisk signs. Positive clones from PCR screening were further verified at the plasmid DNA level by PCR and DNA sequencing. The cloning and PCR screening assays were repeated at least in three different batches of experiments. Representative results are shown.

this system usually requires construction of multiple vectors to achieve effective knockdown when multiple siRNA sites are desired. Thus, we later took the advantage of the Gibson DNA assembly technique and developed a simplified one-step assembly system, the so-called pSOK system, for engineering a single vector that expresses multiple siRNA target sites.[14] While we and others have successfully used the pSOK system and carried out numerous siRNA-based studies,[15−22] the Gibson DNA assembly technique is highly empirical and not user-friendly for researchers with average experience in molecular cloning.

Here, we sought to develop a more user-friendly system to accomplish multiplex siRNA expression in a single vector. Specifically, by taking the advantage of a unique feature of restriction endonuclease BstXI, we developed a modular BstXI-based shotgun cloning (BSG) system that consists of three entry vectors with three siRNA expression units (SiEUs) flanked with four distinct BstXI sites, allowing shotgun assembly of multiple SiEUs simultaneously in a retroviral destination vector. To demonstrate the user-friendliness, technical feasibility, and functionality of the BSG system, we carried out three series of proof-of-principle studies by engineering multiplex siRNA vectors that silence mouse β-catenin, mouse Smad4, or both β-catenin and Smad4, respectively, and tested their functionalities in mesenchymal stem cells (MSCs) iMEFs. We demonstrated that a mix of three siRNA cassettes were

DOI: 10.1021/acssynbio.9b00203
ACS Synth. Biol. 2019, 8, 2092−2105

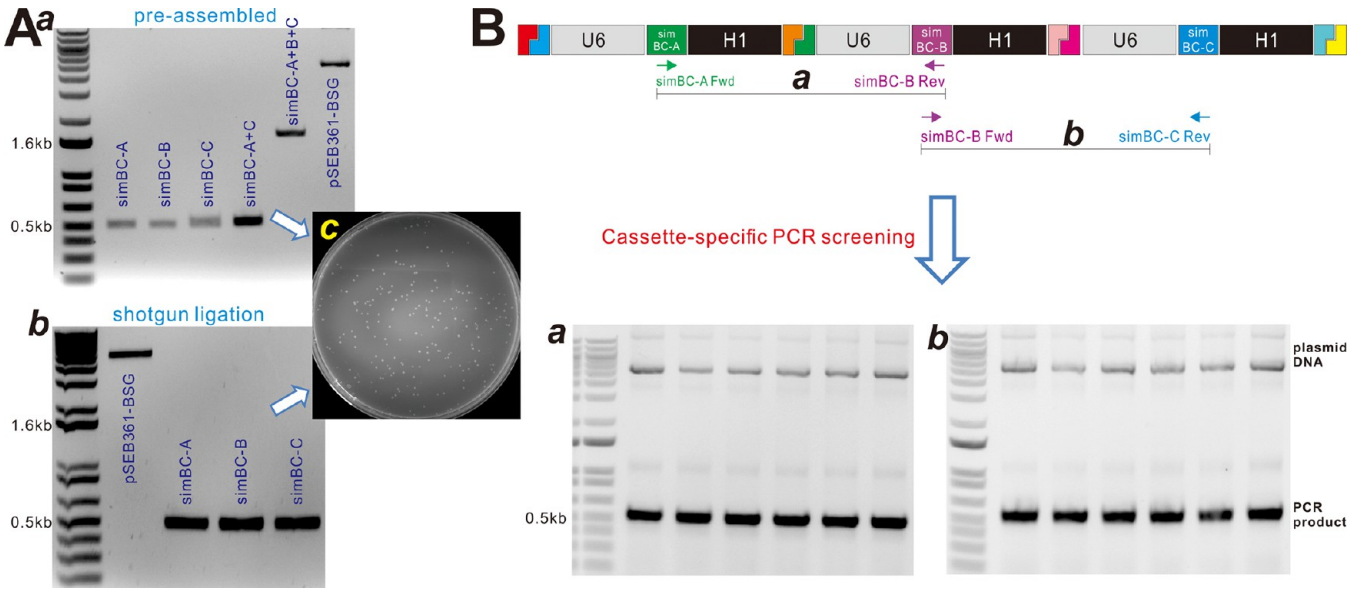

Figure 3. BstXI-based shotgun assembly of three simBC expression units into pSEB361-BSG destination vector. (A) Two approaches for assembling the three simBC SiEUs. In the first approach, the prepared three simBC SiEUs were mixed and preligated to yield the simBC-A+B+C fragment before being cloned into the BstXI-digested pSEB361-BSG (a). Note that simBC-A and simBC-C failed to form a simBC-A+C fragment due to incompatible BstXI ends. Alternatively, the prepared three simBC SiEUs were pooled and ligated into the BstXI-digested pSEB361-BSG (b). Both approaches yield robust numbers of colonies upon bacterial transformation (c). (B) PCR confirmation of the presence of three simBC expression units in the BstXI-based shotgun assembly in pSEB361-simBC. Six potential pSEB361-simBC clones (in plasmid DNA form) were PCR verified with two pairs of simBC-specific primers: (a) simBC-A forward and simBC-B reverse, and (b) simBC-B forward and simBC-C reverse. The selected six clones were positive for both PCR primer sets.

effectively cloned into respective entry vectors through a shotgun approach. Furthermore, the pooled BstXI-released SiEU fragments could be specifically and effectively assembled seamlessly in a defined order at distinct BstXI sites into the retroviral destination vector using the one-step shotgun approach. We demonstrated that the target genes, mouse β-catenin, Smad4, or β-catenin and Smad4, were effectively silenced by the multiplex siRNAs. Furthermore, we found that stable expression of these multiplex siRNAs in MSCs significantly inhibited the pathway-specific reporter activities and the Wnt3A or BMP9-induced expression of downstream target genes. Furthermore, we demonstrated that silencing β-catenin, Smad4, or both β-catenin and Smad4 significantly diminished the Wnt3A and/or BMP9-induced osteogenic differentiation of MSCs *in vitro* and *in vivo*. Collectively, these results demonstrate that the BSG system provides a highly simplified and user-friendly method to express multiplex siRNAs in a single vector for silencing one gene or multiple genes, and thus should be a valuable tool for gene function studies and the development of experimental therapeutics.

RESULTS AND DISCUSSION

Development of a Versatile BstXI-Based Shotgun (BSG) Cloning System for Multiplex siRNA Expression in a Single Vector. Restriction endonuclease BstXI recognizes the 12-bp sequence CCANNNNNNTGG, which contains six undefined base pairs flanked by three defined palindromic sequences (Figure 1A,a). By taking advantage of the unique feature of BstXI sites, we engineered four distinct BstXI sites, namely BstXI-A (CCA*AGTTGG*TGG), BstXI-B (CCA*GCCCTG*TGG), BstXI-C (CCA*TTGCTC*TGG), and BstXI-D (CCA*CCTACA*TGG), each of which, upon BstXI digestion, yields unique and nonpalindromic overhangs for specific complementary sequence-based ligation (underlined and italicized).

We first sought to construct a series of entry vectors, which contain modular siRNA expression units (SiEUs), and are flanked with distinct BstXI sites (Figure 1A,b). We have demonstrated that the convergent U6 and H1 promoters can effectively drive siRNA expression from an oligonucleotide cassette.[13,14,16,19,23−25] To ensure high specificity during shotgun ligations, we engineered unique restriction sites for each oligo cassette and SiEU (Figure 1B). As a proof-of-principle study, we designed three BstXI-based shotgun (BSG) entry vectors, namely pBSG361A, pBSG361B, and pBSG361C for cloning individual siRNA cassettes (Figure 1B, and Supplemental Figure 1A, 1B, and 1C). The one-step assembly of BstXI-digested multiple SiEUs can be then carried out through shotgun ligation at distinct BstXI sites (e.g., BstXI-A through BstXI-D), generating a retroviral multiplex siRNA expression (destination) vector, pSEB361-siRNA (ABC) (Figure 1C,a,b, and Supplemental Figure 1D). It is conceivable that more than three SiEUs can be included in this system, as long as additional distinct BstXI sites are engineered. However, in this case more entry vector(s) with unique BstXI overhangs need to be engineered. Furthermore, the cloning efficiency is expected to decrease when more fragments are ligated into a single vector. Nonetheless, the BSG system is a highly versatile system to simultaneously express multiple siRNAs.

Shotgun Cloning of Three siRNAs Targeting Mouse β-Catenin (simBC) Using the BSG Vector System. To demonstrate the technical feasibility of the BstXI-based shotgun cloning system, we designed three siRNAs targeting mouse β-catenin (i.e., simBC-A/B/C) as one of the proof-of-principle experiments (Figure 2A). It is been well established that β-catenin is an essential mediator/regulator of the canonical Wnt signaling pathway.[26−30] For shotgun ligations, the three

DOI: 10.1021/acssynbio.9b00203
ACS Synth. Biol. 2019, 8, 2092−2105

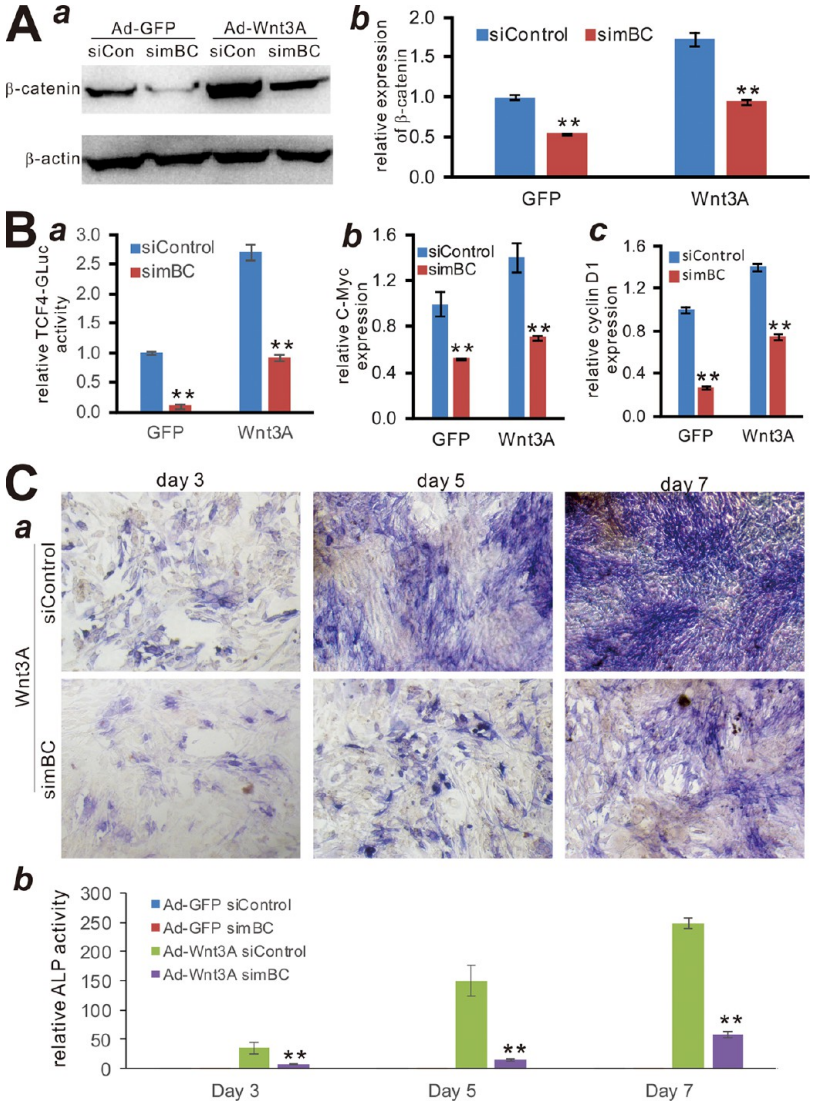

Figure 4. Silencing mouse *β*-catenin by pSEB361-simBC effectively suppresses Wnt3A-induced osteogenic differentiation of mesenchymal stem cells (MSCs). (A) pSEB361-simBC effectively knocks down *β*-catenin expression and prevents Wnt3A-induced increase of *β*-catenin in MSCs. The pSEB361-simBC was used to package retrovirus for establishing the stable MSC line iMEF-simBC, while a scrambled pSEB361-siControl was used to generate the control line iMEF-siControl. Both cell lines were infected with Ad-GFP or Ad-Wnt3A for 72h. (a) The infected cells were lysed and the total cell lysate was subjected to Western blotting analysis with an anti-*β*-catenin antibody. *β*-Actin expression was used as a loading control. (b) The infected cells were also used for total RNA isolation, followed by TqPCR analysis of *β*-catenin expression (*Gapdh* as a reference gene). Double asterisks (**) indicate $p < 0.01$, the simBC group vs the siControl group. (B) Silencing *β*-catenin suppresses Tcf4/LEF reporter activity and the expression of *β*-catenin downstream target genes c-Myc and cyclin D1. (a) The iMEF-simBC and iMEF-siControl cells were transfected with pBGluc-Tcf4/LEF reporter and infected with Ad-Wnt3A or Ad-GFP. At 48 h after transfection, the culture supernatants were collected for Gaussia luciferase assays. (b,c) Subconfluent iMEF-simBC and iMEF-siControl cells were infected with Ad-Wnt3A or Ad-GFP for 72 h. Total RNA was isolated from the infected cells and subjected to TqPCR analysis of c-Myc (*b*) and cyclin D1 (*c*) expression. Double asterisks (**) indicate $p < 0.01$, the simBC group vs the siControl group. (C) Silencing *β*-catenin expression diminishes Wnt3A-induced osteogenic differentiation of MSCs. Subconfluent iMEF-simBC and iMEF-siControl cells were infected with Ad-Wnt3A or Ad-GFP. At days 3, 5, and 7 after infection, the infected cells were subjected to qualitative histochemical staining assay (a) and quantitative bioluminescent assay (b) of the early osteogenic marker ALP. Representative images are shown. Double asterisks (**) indicate $p < 0.01$, the simBC group vs the siControl group.

pBSG361 entry vectors were digested with BstXI and mixed together as the vector pool, while the three annealed simBC oligo cassettes were mixed at equal molar concentration as the pooled inserts. Conventional ligations were performed (NEB), and the ligation products were transformed into electro-competent DH10B cells via electroporation, yielding an average of about 200 colonies per plate (Figure 2A). Bacterial colonies were PCR screened with siRNA-specific primers for simBC-A, simBC-B, or simBC-C, which yielded approximately 30−40% positivity for each SiEU (Figure 2B), indicating that the shotgun cloning of the simBC cassettes is effective and specific.

Next, we sought to carry out a second round of shotgun cloning to assemble the three simBC expression modules into the pSEB361-BSG destination vector. To test ligation efficiency and specificity of the BstXI-digested simBC SiEUs, we first tested if the three SiEUs could be effectively assembled and ligated to the pSEB361-BSG vector. We found that simBC-A/B/C fragments (about 0.5kb each) were effectively ligated to form an expected ~1.5kb product (Figure 3A,a). As expected, simBC-

DOI: 10.1021/acssynbio.9b00203
ACS Synth. Biol. 2019, 8, 2092−2105

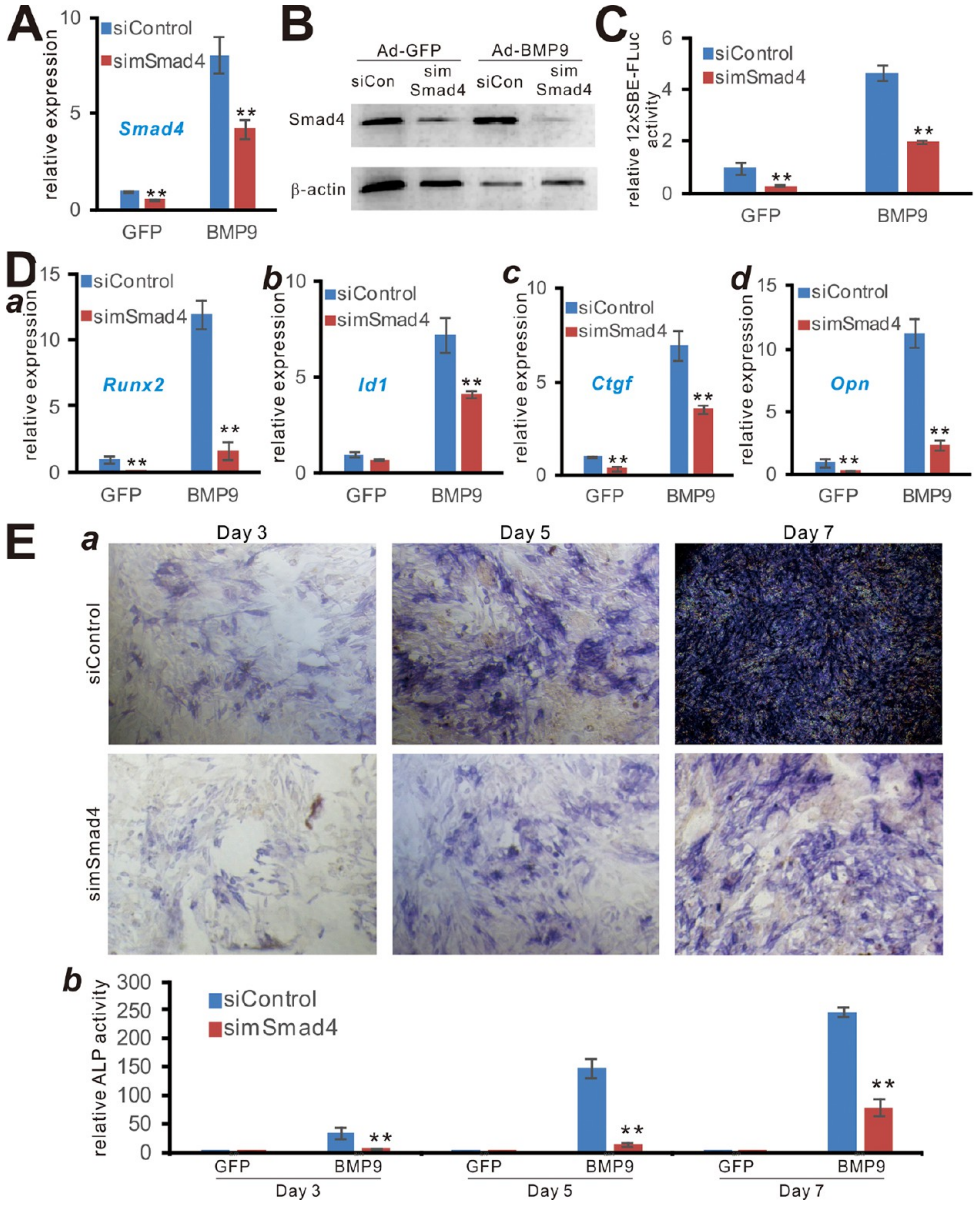

Figure 5. Silencing mouse Smad4 (simSmad4) effectively inhibits BMP9-induced osteogenic differentiation of MSCs. (A) pSEB361-simSmad4 effectively knocks down Smad4 expression in MSCs. The retroviral vector pSEB361-simSmad4 was used to establish the stable MSC line iMEF-simSmad4 (iMEF-siControl as a control). Both cell lines were infected with Ad-GFP or Ad-BMP9 for 72 h. Total RNA was isolated and subjected to TqPCR analysis of Smad4 expression (*Gapdh* as a reference gene). Double asterisks (**) indicate $p < 0.01$, the simSmad4 group vs the siControl group. (B) The iMEF-simSmad4 and iMEF-siControl cells were infected with Ad-GFP or Ad-BMP9 for 72 h, and were lysed and subjected to Western blotting analysis with an anti-Smad4 antibody. β-Actin expression was used as a loading control. (C) Silencing Smad4 suppresses BMPR-Smad reporter 12xSBE-Luc activity in MSCs. The iMEF-simBC and iMEF-siControl cells were transfected with the 12xSBE-Luc reporter and infected with Ad-BMP9 or Ad-GFP. At 48 h after transfection, the cells were lysed and subjected to firefly luciferase activity assay. Double asterisks (**) indicate $p < 0.01$, the simSmad4 group vs the siControl group. (D) Silencing Smad4 suppresses BMP9-induced expression of downstream target genes in MSCs. The cDNA samples prepared in panel A were further subjected to TqPCR analysis of Runx2 (a), Id1 (b), Ctgf (c), and Opn (d) expression, while *Gapdh* served as a reference gene. Double asterisks (**) indicate $p < 0.01$, the simBC group vs the siControl group. (E) Silencing Smad4 expression inhibits BMP9-induced osteogenic differentiation of MSCs. Subconfluent iMEF-simSmad4 and iMEF-siControl cells were infected with Ad-BMP9 or Ad-GFP. At days 3, 5, and 7 after infection, the infected cells were subjected to qualitative histochemical staining assay (a) and quantitative bioluminescent assay (b) of the early osteogenic marker ALP. Representative images are shown. Double asterisks (**) indicate $p < 0.01$, the simSmad4 group vs the siControl group.

A and simBC-C failed to form any larger ligation product, indicating that the distinct BstXI site-mediated ligations are not only effective but also specific. In an alternative approach, we directly set up a ligation reaction using a mix of the BstXI-digested pSEB361-BSG destination vector and the pooled simBC-A/B/C fragments (Figure 3A,b). Both ligation approaches yielded approximately similar numbers of colonies upon bacterial transformation (Figure 3A,c). Using the simBC site-specific primer pairs for simBC-A/simBC-B and simBC-B/simBC-C we were able to confirm the presence of all three simBC SiEUs in the final construct, namely pSEB361-simBC (Figure 3Ba,b).

Silencing Mouse β-Catenin by pSEB361-simBC Effectively Suppresses Wnt3A-Induced Osteogenic Differ-

DOI: 10.1021/acssynbio.9b00203
ACS Synth. Biol. 2019, 8, 2092−2105

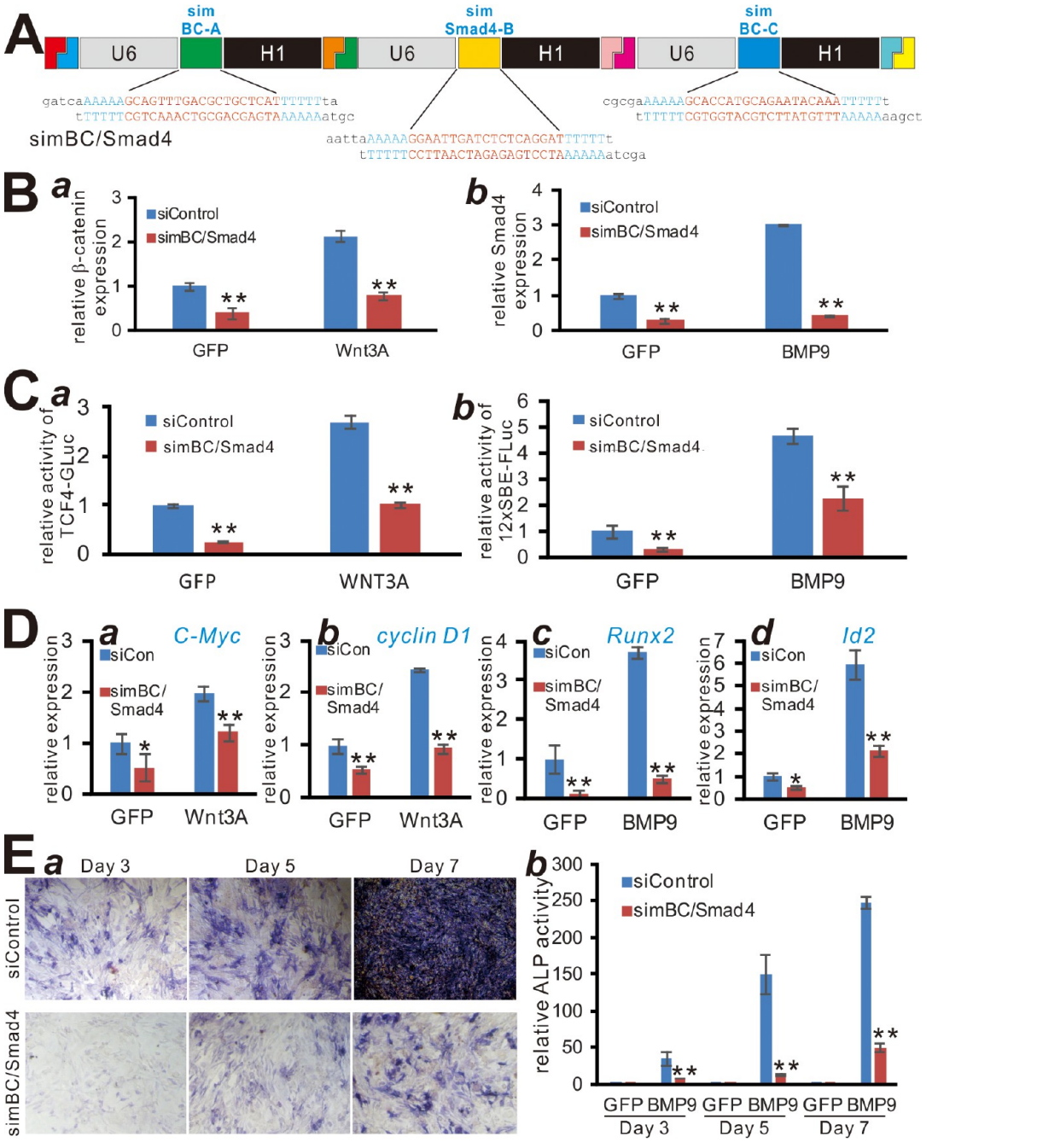

Figure 6. Simultaneous silencing of β-catenin and Smad4 (simBC/Smad4) effectively diminishes Wnt3A and BMP9-induced osteogenic differentiation of MSCs. (A) Schematic representation of the pSEB361-simBC/Smad4 multiplex siRNA construct, which contains two modular units of mouse β-catenin siRNAs (i.e., simBC-A and simBC-C) and one module of mouse Smad4 siRNA (i.e., simSmad4-B). The siRNA sites are highlighted in red letters. (B) The simBC/Smad4 construct effectively knocks down the expression of both β-catenin and Smad4 in MSCs. The stable lines iMEF-simBC/Smad4 and iMEF-siControl were infected with Ad-GFP, Ad-Wnt3A, or Ad-BMP9 for 72 h. Total RNA was isolated and subjected to TqPCR analysis of β-catenin (a) or Smad4 (b) expression (*Gapdh* as a reference gene). Double asterisks (**) indicate $p < 0.01$, the simBC/Smad4 group vs the siControl group. (C) The simBC/Smad4 construct suppresses both β-catenin/Tcf4 and BMPR-Smad reporter activities in MSCs. Subconfluent iMEF-simBC/Smad4 and iMEF-siControl cells were transfected with Tcf4/LEF-GLuc or 12xSBE-Luc reporter plasmid, and infected with Ad-GFP, Ad-Wnt3A, or Ad-BMP9 for 48 h. Tcf4/LEF-GLuc reporter assays were done by measuring GLuc activity in the culture medium (a), while 12xSBE-Luc reporter activities were determined by lysing the cells for firefly luciferase activity assays (b). Double asterisks (**) indicate $p < 0.01$, the simBC/Smad4 group vs the siControl group. (D) The simBC/Smad4 construct effectively suppresses the target gene expression of both Wnt/β-catenin and BMPR-Smad signaling pathways in MSCs. Subconfluent iMEF-simBC/Smad4 and iMEF-siControl cells were infected with Ad-GFP, Ad-Wnt3A, or Ad-BMP9 for 48 h. Total RNA was isolated for TqPCR analysis for the expression of c-Myc (a) and cyclin D1 (b), Runx2 (c), and Id2 (d) by Wnt3A and BMP9, respectively. *Gapdh* was used as a reference gene. Double asterisks (**) indicate $p < 0.01$, simBC/Smad4 group vs siControl group. (E) The simBC/Smad4 construct effectively inhibits BMP9-induced ALP activity in MSCs. Subconfluent iMEF-simBC/Smad4 and iMEF-siControl cells were infected with Ad-GFP or Ad-BMP9. At the indicated time points, the cells were fixed and subjected to the histochemical staining assay for ALP activity (a). Alternatively, the infected iMEFs were lysed at the indicated time points, and subjected to quantitative bioluminescent assay (b). Double asterisks (**) indicate $p < 0.01$, simBC/Smad4 group vs siControl group.

DOI: 10.1021/acssynbio.9b00203
ACS Synth. Biol. 2019, 8, 2092−2105

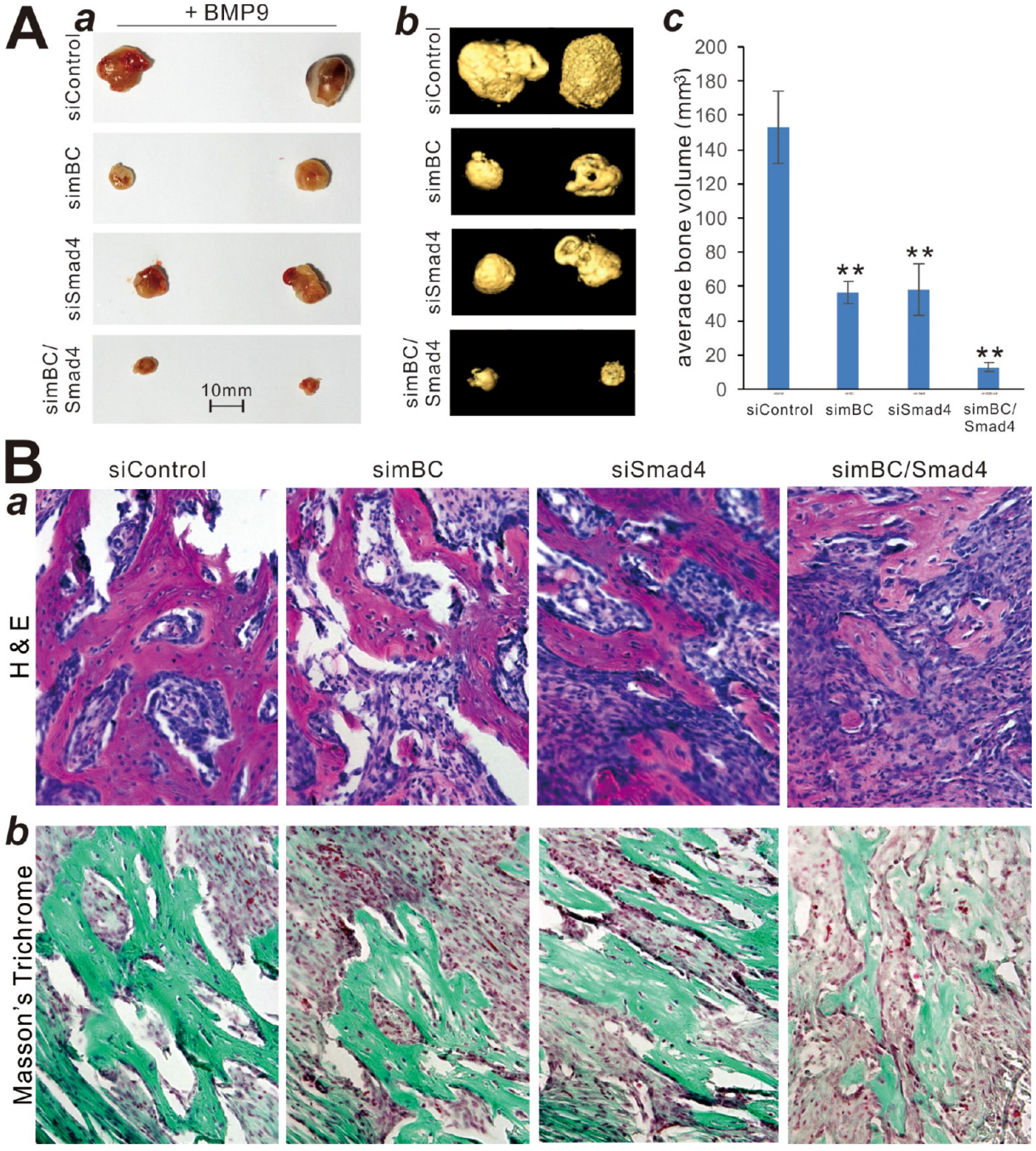

Figure 7. Silencing β-catenin and/or Smad4 in MSCs significantly diminishes BMP9-induced ectopic bone formation *in vivo*. (A) The effect of silencing of β-catenin and/or Smad4 in MSCs on BMP9-induced ectopic bone formation *in vivo*. Exponentially growing iMEF-simBC, iMEF-simSmad4, iMEF-simBC/Smad4, and iMEF-siControl cells were infected with Ad-BMP9 or Ad-GFP for 36 h, and collected for subcutaneous injection into the flanks of athymic nude mice (n = 5 per group). At 5 weeks after implantation, animals were sacrificed, and bony masses at the injection sites were retrieved. Representative gross images are shown (a). No detectable masses were retrieved from the GFP group. The retrieved masses were subjected to microCT imaging, and representative results of the 3-D reconstruction of scanning are shown (b). The average bone volumes of the retrieved bony masses were quantitatively analyzed by using the Amira software (c). Double asterisks (**) indicate $p < 0.01$, siRNA groups vs siControl group. (B) Histology and trichrome staining. The retrieved samples were decalcified and subjected to hematoxylin and eosin staining (a) and Masson's Trichrome staining (b). Representative images are shown.

entiation of Mesenchymal Stem Cells (MSCs). We next evaluated the effect of multiplex β-catenin siRNA expression on the biological functions of Wnt/β-catenin as we and others have demonstrated that canonical Wnt signaling plays an important role in osteogenic lineage differentiation in MSCs.[21,29,31−34] We first established the iMEF-simBC and iMEF-siControl stable lines. Western blotting analysis showed that simBC expression effectively reduced β-catenin expression and prevented Wnt3A-induced elevation of β-catenin at the protein level (Figure 4A,a). Similar results were obtained from qPCR analysis of β-catenin expression in the iMEF cells (Figure 4A,b). Furthermore, silencing β-catenin by simBC diminished Wnt3A-induced Tcf4/LEF reporter activity (Figure 4B,a), and inhibited the expression of Wnt3A-induced Wnt/β-catenin target genes, c-Myc and

DOI: 10.1021/acssynbio.9b00203
ACS Synth. Biol. 2019, 8, 2092−2105

cyclin D1 (Figure 4B,b,c).[32,35−37] Silencing β-catenin by simBC significantly inhibited, both qualitatively and quantitatively, Wnt3A-induced activities of the osteogenic marker alkaline phosphatase (ALP) in MSCs (Figure 4C,a,b). Collectively, these results demonstrate that multiplex β-catenin siRNA expression with the BSG vector system effectively silences mouse β-catenin and inhibits its biological functions in MSCs.

Silencing Mmouse Smad4 (simSmad4) Using the BSG Vector System Effectively Inhibits BMP9-Induced Osteogenic Differentiation of MSCs. We carried out the second proof-of-principle experiment by constructing a multiplex siRNA targeting mouse Smad4, or simSmad4, using the BSG vector system. Smad4 is an essential signaling mediator of TGF-β and BMP signaling pathways.[38−40] We showed that the simSmad4 effectively silenced endogenous Smad4 and prevented BMP9-induced Smad4 expression both at mRNA and protein levels (Figure 5A,B). Accordingly, BMP9-stimulated 12xSBE-FLuc BMP-R Smad reporter activity was effectively inhibited in the iMEF-simSmad4 cells, compared with that of the iMEF-siControl cells ($p < 0.01$) (Figure 5C). Therefore, these results confirm that multiplex Smad4 siRNA expression with the BSG vector system effectively silences mouse Smad4 expression in MSCs.

We further examined the biological consequence of Smad4 knockdown in MSCs by evaluating the effect of simSmad4 on the well-characterized BMP9 target genes.[33,41−43] We found that silencing Smad4 by simSmad4 markedly decreased the BMP9-induced expression of Runx2, Id1, Ctgf, and osteopontin (Opn) (Figure 5D,a−d). Even though BMP9 is one of the most potent osteogenic BMPs,[24,40,44−48] simSmad4 significantly inhibited BMP9-induced ALP activity in MSCs both qualitatively and quantitatively (Figure 5E,a,b). Thus, the above results demonstrate that multiplex Smad4 siRNA expression using the BSG vector system effectively silences mouse Smad4 and inhibits BMP9-induced osteogenic differentiation of MSCs.

Simultaneous Silencing of β-Catenin and Smad4 (simBC/Smad4) Effectively Diminishes Wnt3A and BMP9-Induced Osteogenic Differentiation of MSCs *in Vitro* and *in Vivo*. To demonstrate the versatile applications of the BSG multiplex siRNA expression system, we constructed the pSEB361-simBC/Smad4 vector, which simultaneously targets both β-catenin and Smad4 (Figure 6A). TqPCR analysis showed that both β-catenin and Smad4 were significantly knocked down in the iMEF-simBC/Smad4 cells, and Wnt3A and BMP9 failed to upregulate the expression of β-catenin and Smad4, respectively (Figure 6B,a,b). Accordingly, Wnt3A failed to effectively activate Tcf4/LEF-GLuc reporter activity, and BMP9-induced 12xSBE-FLuc activity was significantly inhibited in the iMEF-simBC/Smad4 cells (Figure 6C,a,b).

Similarly, Wnt3A-upregulated expression of C-Myc and cyclin D1 was inhibited in the iMEF-simBC/Smad4 cells, while silencing both β-catenin and Smad4 in MSCs drastically decreased BMP9-induced expression of Runx2 and Id2 (Figure 6D,a−d). Furthermore, BMP9-induced osteogenic marker ALP activity decreased significantly in the iMEF-simBC/Smad4 cells, compared with that of the iMEF-siControl cells (Figure 6D,a,b).

Lastly, we conducted an *in vivo* study to evaluate the effect of silencing β-catenin or Smad4 alone or in combinations via the BSG multiplex siRNA expression system on BMP9-induced bone formation from MSCs. When the iMEF stable lines were infected with Ad-BMP9 or Ad-GFP, and implanted subcutaneously into athymic nude mice for 5 weeks, we found that silencing either β-catenin, Smad4, or both β-catenin and Smad4 in MSCs resulted in significantly diminished bone formation by gross examination, microCT imaging, and quantitative average bone volume analysis, compared with that of the control group (e.g., the iMEF-siControl cells) (Figure 7A,a−c). As expected, a simultaneous knockdown of both β-catenin and Smad4 led to the greatest decrease in ectopic bone formation, compared with either silencing β-catenin or Smad4 alone (Figure 7A). H&E histologic evaluation further demonstrated that silencing either β-catenin, Smad4, or both in MSCs resulted in a significant decrease in the number and thickness of trabecular bone, compared with that of the siControl group (Figure 7B,a). Masson's trichrome staining further revealed that there was a significant decrease in mature and fully mineralized bone matrix in the β-catenin, Smad4, or both knockdown groups, compared with that of the siControl group (Figure 7B,b). Collectively, the above *in vivo* results further substantiate our *in vitro* findings, and demonstrate that multiplex siRNAs expressed by the BSG shotgun system are highly effective in targeting one gene or multiple genes in mammalian cells.

The BstXI-Based Modular siRNA Expression System Provides a Flexible and Versatile Platform for Efficient Multiplex Gene Silencing. To overcome the technical challenges in simultaneously expressing multiple siRNAs in a single vector to accomplish silencing a specific gene or different genes, here, we developed a modular BstXI-based shotgun cloning (BSG) system that consists of three siRNA expression units (SiEUs) flanked with four distinct BstXI sites, allowing shotgun assembly of multiple SiEUs simultaneously. In fact, the BSG system employs two stages of shotgun cloning. The first step involved in shotgun cloning of individual siRNA oligo cassettes into respective SiEU vectors at unique restriction sites. The second shotgun-cloning step is to assemble individual SiEUs into the retroviral destination vector at distinct BstXI sites.

To demonstrate the user-friendliness, technical feasibility, and functionality of the BSG system, we carried out three sets of proof-of-principle studies by engineering multiplex siRNA vectors that silence the expression of mouse β-catenin (simBC), mouse Smad4 (simSmad4), or both β-catenin and Smad4 (simBC/Smad4) in mesenchymal stem cells iMEFs, respectively. Our results indicate that a mix of individual siRNA cassettes were effectively cloned into respective pBSG361 vectors through a shotgun approach. A mix of BstXI-released SiEU fragments can then be specifically and effectively assembled at distinct BstXI sites with one-step ligation into the distinct BstXI sites of the destination retroviral vector pSEB361-BSG. We demonstrated that the target genes, mouse β-catenin, Smad4, or β-catenin and Smad4, were effectively silenced by the multiplex siRNAs. Furthermore, we found that stable expression of these multiplex siRNAs in MSCs significantly inhibited the pathway-specific reporter activities and the expression of well-established downstream target genes for Wnt3A and/or BMP9, respectively. Furthermore, we demonstrated that silencing β-catenin, Smad4, or both β-catenin and Smad4 significantly diminished the Wnt3A and/or BMP9-induced osteogenic differentiation of MSCs *in vitro* and *in vivo*. Collectively, these results demonstrate that the BSG system provides a rapid, simplistic, and user-friendly method to express multiplex siRNAs for efficient knockdown of one gene or multiple genes.

It is conceivable that the reported BSG system can be easily customized to accommodate more than three SiEUs if more distinct BstXI sites are designed, which provides another layer of

DOI: 10.1021/acssynbio.9b00203
ACS Synth. Biol. 2019, 8, 2092−2105

flexibility and variability to expand siRNA targeting complexity. Furthermore, the reported BSG system can be easily configured for lentiviral, adenoviral, and/or adeno-associated viral (AAV) vector systems. In these cases, viral vector-specific destination vectors need to be constructed, while the same entry vectors can be used. Such potential further highlights the versatility of the BSG system in expressing multiplex siRNAs in mammalian cells.

The development of an effective siRNA delivery and expression system is attractive and beneficial to the scientific community. By employing the Gibson DNA Assembly technology, we previously developed a one-step system, so-called pSOK system, to simultaneously express multiple siRNAs that silence one specific gene or different genes in a single vector.[14] We and others successfully used this system and carried out numerous siRNA-based studies.[15−22] However, the Gibson DNA Assembly methodology is rather finicky and highly empirical. In fact, vectors containing more than two siRNAs were less effectively assembled under the reported assembly condition. Therefore, while the pSOK system is working robustly for experienced molecular biologists, this system is not user-friendly for researchers with average experience in molecular cloning. In this report, we have developed a better and more user-friendly system to accomplish multiplex siRNA expression in mammalian cells.

It is conceivable that the BSG system can be further modified for expressing multiplex sgRNAs in a single vector for CRISPR/Cas9-based genome editing studies.[49−52] Nonetheless, other strategies for single-vector-based multiplex siRNA and/or sgRNA expression should be explored. Similar to our pSOK system for siRNA expression,[14] Breunig et al. reported a so-called STAgR (string assembly gRNA cloning) technique, which is a single step gRNA multiplexing system by taking the advantage of the N20 targeting sequences as necessary homologies for Gibson Assembly.[53] More recently, Zukermann et al. developed an elaborate procedure that allows the assembly of multiple gRNA expression cassettes into a vector of choice within a single step, or so-called ASAP (adaptable system for assembly of multiplexed plasmids)-cloning.[54] This ASAP-cloning system combined the "PCR-on-ligation" step for flexible generation of individual insert fragments and the utilization of pairs of isocaudomers for ligation of the generated inserts into type II restriction endonuclease sites in common expression vectors.[54] While these systems can be modified for siRNA expression, such modifications are more technically challenging as siRNAs require the expression of both strands, which is not the case of sgRNA expression.

In summary, we developed a simplified and versatile BstXI-based shotgun (or BSG) cloning system for a rapid generation of multiplex siRNA expression in a single-vector. We carried out three series of proof-of-principle studies and engineered multiplex siRNA vectors to silence the expression of mouse β-catenin, mouse Smad4, or both β-catenin and Smad4. Experimentally, we demonstrated that distinct siRNA expression units can be assembled seamlessly in a defined order into the destination vector using one-step shotgun approach. Our *in vitro* studies revealed that the multiplex siRNA expression mediated by BSG single vectors effectively silenced β-catenin, Smad4, or both β-catenin and Smad4, and inhibited the Wnt3A and/or BMP9 signaling activities, as well as blunting BMP9-induced osteogenic differentiation of MSCs *in vivo*. The BSG system can be easily customized to accommodate the expression of more than three siRNAs, offering more flexibility and variability to expand siRNA targeting complexity. Taken together, our results demonstrate that the BSG system provides a rapid and user-friendly method to express multiplex siRNAs in a single vector and thus should be a valuable tool for gene function studies and the development of therapeutics.

MATERIALS AND METHODS

Cell Culture and Chemicals. HEK-293 cells were obtained from the American Type Culture Collection (ATCC, Manassas, VA). HEK-293 derivative lines 293pTP and 293 RAPA cells were previously characterized.[55,56] Mouse mesenchymal stem cell (MSC) line iMEFs was previously characterized.[57,58] All cell lines were maintained in DMEM supplemented with 10% fetal bovine serum (FBS, Gemini Bio-Products, West Sacramento, CA), containing 100 U/mL penicillin and 100 μg/mL streptomycin, at 37 °C in 5% CO_2 as described.[21,59,60] All restriction endonuclease enzymes were purchased from New England Biolabs (NEB, Ipswich, MA). Blasticidin S was purchased from InvivoGen (San Diego, CA). Unless indicated otherwise, other reagents were purchased from Sigma-Aldrich (St. Louis, MO) or Thermo Fisher Scientific (Waltham, MA).

Construction of BstXI-Based Shotgun (BSG) Multiplex siRNA Expression System. The entry vectors pBSG361A/B/C were first engineered on the base of pBR322 plasmid so that each vector contains the converging U6−H1 promoters to drive siRNA expression, as previously described,[13,14] with unique restriction sites for the subcloning of siRNA oligo cassettes (SiOCs), whereas the U6−H1-driven siRNA expression units (SiEUs) were flanked with a pair of distinct BstXI sites, namely BstXI-A and BstXI-B in pBSG361A, BstXI-B and BstXI-C in pBSG361B, and BstXI-C and BstXI-D in pBSG361C, respectively (Supplemental Figure 1A−1C). A retroviral destination vector, pSEB361-BSG, was also engineered for shotgun cloning of multiple BstXI-digested SiEUs from the pBSG361 vectors at the BstXI-A and BstXI-D sites (Supplemental Figure 1D).

The siRNA sites targeting the coding regions of mouse β-catenin (NM_007614.3) and Smad4 (NM_008540.3) were designed by using the *BLOCK-iT RNAi Designer* (Invitrogen, Carlsbad, CA) and/or the *siDESIGN* programs (Dharmacon, Lafayette, CO), as previously described.[14,16−18] Three scrambled oligo sequences, which do not target any significant known human and rodent transcripts, were used as controls, or siControl. The annealed siRNA oligo cassettes (Supplemental Table 1) were used for shotgun cloning into the pBSG361 entry vectors. The resulting constructs were designated as pBSG361-simBC-A/B/C (for mouse β-catenin siRNAs) and pBSG361-simSmad4-A/B/C (for mouse Smad4 siRNAs), as well as pBSG361-simBC/Smad4 for the dual targeting siRNAs of β-catenin/Smad4, and pBSG361-siControl. To construct a multiplex siRNA expression retroviral vector, the three corresponding SiEUs were isolated from pBSG361 vectors by BstXI digestion, and pooled for shotgun ligation into the BstXI-A/BstXI-D sites of the pSEB361-BSG retroviral vector. All cloned oligo cassettes were verified by DNA sequencing. Details about the construction of these vectors and related vector sequences are available upon request.

Establishment of Stable siRNA Expressing Cell Lines of Mesenchymal Stem Cells iMEFs. The retroviral transfer vectors pSEB361-simBC, pSEB361-simSmad4, pSEB361-simBC/Smad4, and pSEB361-siControl were cotransfected with retroviral packaging plasmids into the 293 Phoenix Ampho (293PA) cells to generate retrovirus supernatants for infecting subconfluent iMEF cells as previously described.[19,61,62]

DOI: 10.1021/acssynbio.9b00203
ACS Synth. Biol. 2019, 8, 2092−2105

At 36−48 h post-viral-infection, the cells were subjected to blasticidin S selection (final concentration at 3 μg/mL) for 5 days. The resultant stable lines were designated as iMEF-simBC, iMEF-simSmad4, iMEF-simBC/Smad4, and iMEF-siControl, respectively.

Generation and Amplification of Recombinant Adenoviruses Ad-Wnt3A, Ad-BMP9, and Ad-GFP. Recombinant adenovirus expressing mouse Wnt3A (i.e., Ad-Wnt3A) or human BMP9 (i.e., Ad-BMP9) was constructed by using the AdEasy system as described.[63−66] These adenoviruses were further amplified in 293pTP or RAPA cells to achieve high titers.[55,56] Ad-Wnt3A and Ad-BMP9 also coexpress GFP as a marker for monitoring infection efficiency. An analogous adenovirus expressing only GFP (i.e., Ad-GFP) was used as a mock virus control.[67] Furthermore, polybrene (aka, hexadimethrine bromide) was added to the culture medium (at final concentration of 5 μg/mL) of adenovirus infection to enhance adenoviral infection efficiency.[68,69]

Total RNA Isolation and Touchdown-qPCR (TqRCR) Analysis. At the indicated time points, total RNA was isolated from the treated cells using TRIZOL Reagent (Invitrogen, Carlsbad, CA, USA) according to the manufacturer's instructions and subjected to reverse transcription as previously described.[70−73] The RT cDNA products were further diluted and used as PCR templates. The qPCR primers were designed by using the Primer3 Plus program (Supplemental Table 1). TqPCR was performed to quantitatively assess the expression levels for the genes of interest as previously described.[67,74,75] The 2xSYBR Green qPCR reactions (Bimake, Houston, TX) were set up according to manufacturer's instructions. *Gapdh* was used as a reference gene. All sample values were normalized to *Gapdh* expression by using the 2-ΔΔCt method.

Bacterial Colony PCR Screening Assay. Ligation products were transformed into aliquots (usually 5−10 μL) of electro-competent DH10B cells (NEB) via electroporation and directly plated onto LB/agar/Kan or Amp plates, as described.[63,76,77] Bacterial colonies were grown for 14−16 h in a 37 °C incubator. Colony PCR was performed as described.[76,77] Briefly, PCR master mix (usually 10−20 μL/reaction) was first aliquoted into a 96-well PCR plate (or multiple 8-tube strips for PCR). At the same time, a replicate of a sterile 96-well cell culture plate was set up by adding ∼50 μL/well LB/Amp or LB/Kap medium. Bacterial colonies were then carefully picked up with sterile p200 pipet tips and loaded onto a 12- or 8-channel pipet. The colony-containing tips were first rinsed gently in the 96-well culture plate loaded with LB/Amp or LB/Kam culture medium, and then rinsed in the corresponding wells of the PCR plate. The LB plate was moved to a 37 °C bacterial incubator, whereas the PCR plate was used for 26−28 cycles of PCR amplification. The PCR products were resolved on 1% agarose gels. Bacterial culture medium corresponding to positive PCR results was grown up for plasmid DNA preparations and further confirmation by PCR, restriction digestion, and/or DNA sequencing.

Alkaline Phosphatase (ALP) Assays. At the indicated time points, ALP activities were assessed either quantitatively by using the modified Great Escape SEAP chemiluminescence assay (Takara Bio USA, Mountain View, CA), and/or qualitatively by using histochemical staining with a mixture of napthol AS-MX phosphate and Fast Blue BB salt, as previously described.[15,23,75] Each assay condition was performed in triplicate. The results were repeated in at least three independent experiments.

Transfection and Gaussia and Firefly Luciferase Reporter Assays. Subconfluent iMEF-derived stable cells were seeded in 25 cm^2 cell culture flasks and transfected with 8 μg/flask of pBGLuc-Tcf4/LEF or p12xSBE-FLuc reporter plasmid using polyethylenimine (PEI) reagents (Polysciences, Inc., Warrington, PA) according to the manufacturer's instructions. At 16 h after transfection, cells were collected, replated into 24-well plates, and infected with compatible titers of Ad-GFP, Ad-Wnt3A, or Ad-BMP9. At the indicated time points after infection, cell culture medium was taken for Gaussia luciferase assay for the pBGLuc-Tcf4/LEF transfected cells, while the cells were lysed for firefly luciferase assays for the p12xSBE-FLuc transfected cells, as previously described.[20,78−81] The luciferase assay kits were purchased from NEB. Each assay condition was performed in triplicate.

Subcutaneous Stem Cell Implantation and Ectopic Bone Formation. The animal use and care involved in this study was approved by the Institutional Animal Care and Use Committee. All experimental procedures were carried out in accordance with the approved guidelines. The subcutaneous iMEFs cell implantation procedure was performed as described.[22,82,83] Specifically, the iMEFs cells were infected with Ad-BMP9 or Ad-GFP for 36 h. The infected cells were harvested, resuspended in sterile PBS (80 μL each injection), and injected subcutaneously into the flanks of athymic nude mice (Envigo/Harlan Research Laboratories; n = 4/group, female, 5−6 week old; 2×10^6 cells per injection site). The animals were maintained ad lib in the biosafety barrier facility. At 5 weeks after implantation, the mice were euthanized, and the implantation sites were retrieved for μCT imaging and histologic evaluation.

Microcomputed Tomographic (μCT) Analysis. The retrieved specimens were fixed in 10% formalin and imaged using the micro-CT (μCT) component of the GE triumph (GE Healthcare, Piscataway, NJ, USA) trimodality preclinical imaging system. The image data were quantitatively analyzed by Amira 5.6 (Visage Imaging, Inc.), and 3-D volumetric data and bone density were determined as previously described.[84−87]

Histologic Staining and Masson's Trichrome Staining. After microCT imaging, the retrieved masses were decalcified and embedded in paraffin. Serial sections of embedded specimens were deparaffinized and subjected to hematoxylin and eosin (H&E) staining and Masson's trichrome staining as described.[21,25,88,89]

Statistical Analysis. All quantitative studies were carried out in triplicate and/or performed in three independent batches. Statistically significant differences between samples were determined by one-way analysis of variance. A value of $p < 0.05$ was defined as statistically significant when a comparison was being made.

■ ASSOCIATED CONTENT

Supporting Information

The Supporting Information is available free of charge on the ACS Publications website at DOI: 10.1021/acssynbio.9b00203.

List of oligonucleotides/primers; vector maps for the BSG system (PDF)

■ AUTHOR INFORMATION

Corresponding Authors

*Tel.: (773) 702-7169. E-mail: tche@uchicago.edu.
*Tel.: (312) 838-0786. E-mail: zengzongyue@126.com.

DOI: 10.1021/acssynbio.9b00203
ACS Synth. Biol. 2019, 8, 2092−2105

ORCID

Tong-Chuan He: 0000-0001-7721-3934

Notes

The authors declare no competing financial interest.

■ ACKNOWLEDGMENTS

The authors are grateful for the technical support provided by the Integrated Small Animal Imaging Research Resource (iSAIRR) Faculty at The University of Chicago. The reported work was supported in part by research grants from the National Key Research and Development Program of China (2016YFC1000803 and 2011CB707906), the National Institutes of Health (CA226303 to T.C.H.), the U.S. Department of Defense (OR130096 to J.M.W.), and the Scoliosis Research Society (T.C.H. and M.J.L.). This project was also supported in part by The University of Chicago Cancer Center Support Grant (P30CA014599) and the National Center for Advancing Translational Sciences of the National Institutes of Health through Grant No. UL1 TR000430. T.C.H. was supported by the Mabel Green Myers Research Endowment Fund and The University of Chicago Orthopaedics Alumni Fund. Funding sources were not involved in the study design; in the collection, analysis, and interpretation of data; in the writing of the report; and in the decision to submit the paper for publication.

■ REFERENCES

(1) Hammond, S. M., Bernstein, E., Beach, D., and Hannon, G. J. (2000) An RNA-directed nuclease mediates post-transcriptional gene silencing in Drosophila cells. *Nature 404* (6775), 293−296.

(2) Setten, R. L., Rossi, J. J., and Han, S. P. (2019) The current state and future directions of RNAi-based therapeutics. *Nat. Rev. Drug Discovery 18* (6), 421−446.

(3) Bobbin, M. L., and Rossi, J. J. (2016) RNA Interference (RNAi)-Based Therapeutics: Delivering on the Promise? *Annu. Rev. Pharmacol. Toxicol. 56*, 103−122.

(4) Castel, S. E., and Martienssen, R. A. (2013) RNA interference in the nucleus: roles for small RNAs in transcription, epigenetics and beyond. *Nat. Rev. Genet. 14* (2), 100−112.

(5) Weng, Y., Xiao, H., Zhang, J., Liang, X. J., and Huang, Y. (2019) RNAi therapeutic and its innovative biotechnological evolution. *Biotechnol. Adv. 37*, 801.

(6) Whitehead, K. A., Langer, R., and Anderson, D. G. (2009) Knocking down barriers: advances in siRNA delivery. *Nat. Rev. Drug Discovery 8* (2), 129−138.

(7) Czech, M. P., Aouadi, M., and Tesz, G. J. (2011) RNAi-based therapeutic strategies for metabolic disease. *Nat. Rev. Endocrinol. 7* (8), 473−484.

(8) Pecot, C. V., Calin, G. A., Coleman, R. L., Lopez-Berestein, G., and Sood, A. K. (2011) RNA interference in the clinic: challenges and future directions. *Nat. Rev. Cancer 11* (1), 59−67.

(9) Fellmann, C., and Lowe, S. W. (2014) Stable RNA interference rules for silencing. *Nat. Cell Biol. 16* (1), 10−18.

(10) de Fougerolles, A., Vornlocher, H. P., Maraganore, J., and Lieberman, J. (2007) Interfering with disease: a progress report on siRNA-based therapeutics. *Nat. Rev. Drug Discovery 6* (6), 443−453.

(11) Iorns, E., Lord, C. J., Turner, N., and Ashworth, A. (2007) Utilizing RNA interference to enhance cancer drug discovery. *Nat. Rev. Drug Discovery 6* (7), 556−568.

(12) Kim, D. H., and Rossi, J. J. (2007) Strategies for silencing human disease using RNA interference. *Nat. Rev. Genet. 8* (3), 173−184.

(13) Luo, Q., Kang, Q., Song, W. X., et al. (2007) Selection and validation of optimal siRNA target sites for RNAi-mediated gene silencing. *Gene 395* (1−2), 160−169.

(14) Deng, F., Chen, X., Liao, Z., et al. (2014) A simplified and versatile system for the simultaneous expression of multiple siRNAs in mammalian cells using Gibson DNA Assembly. *PLoS One 9* (11), e113064.

(15) Huang, X., Wang, F., Zhao, C., et al. (2019) Dentinogenesis and Tooth-Alveolar Bone Complex Defects in BMP9/GDF2 Knockout Mice. *Stem Cells Dev. 28* (10), 683−694.

(16) Yan, S., Zhang, R., Wu, K., et al. (2018) Characterization of the essential role of bone morphogenetic protein 9 (BMP9) in osteogenic differentiation of mesenchymal stem cells (MSCs) through RNA interference. *Genes Dis. 5* (2), 172−184.

(17) Liao, J., Wei, Q., Zou, Y., et al. (2017) Notch Signaling Augments BMP9-Induced Bone Formation by Promoting the Osteogenesis-Angiogenesis Coupling Process in Mesenchymal Stem Cells (MSCs). *Cell. Physiol. Biochem. 41* (5), 1905−1923.

(18) Liao, J., Yu, X., Hu, X., Fan, J., Wang, J., Zhang, Z., Zhao, C., Zeng, Z., Shu, Y., Zhang, R., et al. (2017) lncRNA H19 mediates BMP9-induced osteogenic differentiation of mesenchymal stem cells (MSCs) through Notch signaling. *Oncotarget. 8* (32), 53581−53601.

(19) Wang, J., Liao, J., Zhang, F., et al. (2017) NEL-Like Molecule-1 (Nell1) Is Regulated by Bone Morphogenetic Protein 9 (BMP9) and Potentiates BMP9-Induced Osteogenic Differentiation at the Expense of Adipogenesis in Mesenchymal Stem Cells. *Cell. Physiol. Biochem. 41* (2), 484−500.

(20) Deng, Y., Wang, Z., Zhang, F., et al. (2016) A Blockade of IGF Signaling Sensitizes Human Ovarian Cancer Cells to the Anthelmintic Niclosamide-Induced Anti-Proliferative and Anticancer Activities. *Cell. Physiol. Biochem. 39* (3), 871−888.

(21) Zhang, H., Wang, J., Deng, F., et al. (2015) Canonical Wnt signaling acts synergistically on BMP9-induced osteo/odontoblastic differentiation of stem cells of dental apical papilla (SCAPs). *Biomaterials 39*, 145−154.

(22) Li, Y., Wagner, E. R., Yan, Z., et al. (2015) The Calcium-Binding Protein S100A6 Accelerates Human Osteosarcoma Growth by Promoting Cell Proliferation and Inhibiting Osteogenic Differentiation. *Cell. Physiol. Biochem. 37* (6), 2375−2392.

(23) Song, D., Zhang, F., Reid, R. R., et al. (2017) BMP9 induces osteogenesis and adipogenesis in the immortalized human cranial suture progenitors from the patent sutures of craniosynostosis patients. *J. Cell Mol. Med. 21* (11), 2782−2795.

(24) Wang, J., Zhang, H., Zhang, W., et al. (2014) Bone morphogenetic protein-9 effectively induces osteo/odontoblastic differentiation of the reversibly immortalized stem cells of dental apical papilla. *Stem Cells Dev. 23* (12), 1405−1416.

(25) Liu, X., Qin, J., Luo, Q., Bi, Y., Zhu, G., Jiang, W., Kim, S. H., Li, M., Su, Y., Nan, G., et al. (2013) Cross-talk between EGF and BMP9 signalling pathways regulates the osteogenic differentiation of mesenchymal stem cells. *J. Cell Mol. Med. 17* (9), 1160−1172.

(26) Yang, K., Wang, X., Zhang, H., et al. (2016) The evolving roles of canonical WNT signaling in stem cells and tumorigenesis: implications in targeted cancer therapies. *Lab. Invest. 96* (2), 116−136.

(27) Zhang, F., Song, J., Zhang, H., et al. (2016) Wnt and BMP Signaling Crosstalk in Regulating Dental Stem Cells: Implications in Dental Tissue Engineering. *Genes Dis. 3* (4), 263−276.

(28) Gao, Y., Huang, E., Zhang, H., et al. (2013) Crosstalk between Wnt/beta-catenin and estrogen receptor signaling synergistically promotes osteogenic differentiation of mesenchymal progenitor cells. *PLoS One 8* (12), e82436.

(29) Kim, J. H., Liu, X., Wang, J., et al. (2013) Wnt signaling in bone formation and its therapeutic potential for bone diseases. *Ther. Adv. Musculoskeletal Dis. 5* (1), 13−31.

(30) Wagner, E., Zhu, G., Zhang, B.-Q., Luo, Q., Shi, Q., Huang, E., Gao, Y., Gao, J.-L., Kim, S., et al. (2011) The therapeutic potential of the Wnt signaling pathway in bone disorders. *Curr. Mol. Pharmacol. 4* (1), 14−25.

(31) Tang, N., Song, W. X., Luo, J., et al. (2009) BMP-9-induced osteogenic differentiation of mesenchymal progenitors requires functional canonical Wnt/beta-catenin signalling. *J. Cell Mol. Med. 13* (8B), 2448−2464.

DOI: 10.1021/acssynbio.9b00203
ACS Synth. Biol. 2019, 8, 2092−2105

(32) Luo, J., Chen, J., Deng, Z. L., et al. (2007) Wnt signaling and human diseases: what are the therapeutic implications? *Lab. Invest. 87* (2), 97−103.
(33) Luo, Q., Kang, Q., Si, W., et al. (2004) Connective tissue growth factor (CTGF) is regulated by Wnt and bone morphogenetic proteins signaling in osteoblast differentiation of mesenchymal stem cells. *J. Biol. Chem. 279* (53), 55958−55968.
(34) Si, W., Kang, Q., Luu, H. H., et al. (2006) CCN1/Cyr61 is regulated by the canonical Wnt signal and plays an important role in Wnt3A-induced osteoblast differentiation of mesenchymal stem cells. *Mol. Cell. Biol. 26* (8), 2955−2964.
(35) He, T. C., Sparks, A. B., Rago, C., et al. (1998) Identification of c-MYC as a target of the APC pathway [see comments]. *Science 281* (5382), 1509−1512.
(36) Tetsu, O., and McCormick, F. (1999) Beta-catenin regulates expression of cyclin D1 in colon carcinoma cells. *Nature 398* (6726), 422−426.
(37) He, T. C., Chan, T. A., Vogelstein, B., and Kinzler, K. W. (1999) PPARdelta is an APC-regulated target of nonsteroidal anti-inflammatory drugs. *Cell 99* (3), 335−345.
(38) Deng, Z. L., Sharff, K. A., Tang, N., et al. (2008) Regulation of osteogenic differentiation during skeletal development. *Front. Biosci., Landmark Ed. 13*, 2001−2021.
(39) Luo, J., Tang, M., Huang, J., et al. (2010) TGFbeta/BMP type I receptors ALK1 and ALK2 are essential for BMP9-induced osteogenic signaling in mesenchymal stem cells. *J. Biol. Chem. 285* (38), 29588−29598.
(40) Wang, R. N., Green, J., Wang, Z., et al. (2014) Bone Morphogenetic Protein (BMP) signaling in development and human diseases. *Genes Dis. 1* (1), 87−105.
(41) Peng, Y., Kang, Q., Cheng, H., et al. (2003) Transcriptional characterization of bone morphogenetic proteins (BMPs)-mediated osteogenic signaling. *J. Cell. Biochem. 90* (6), 1149−1165.
(42) Peng, Y., Kang, Q., Luo, Q., et al. (2004) Inhibitor of DNA binding/differentiation helix-loop-helix proteins mediate bone morphogenetic protein-induced osteoblast differentiation of mesenchymal stem cells. *J. Biol. Chem. 279* (31), 32941−32949.
(43) Luther, G., Wagner, E., Zhu, G., Kang, Q., Luo, Q., Lamplot, J., Bi, Y., Luo, X., Luo, J., Teven, C., et al. (2011) BMP-9 induced osteogenic differentiation of mesenchymal stem cells: molecular mechanism and therapeutic potential. *Curr. Gene Ther. 11* (3), 229−240.
(44) Cheng, H., Jiang, W., Phillips, F. M., et al. (2003) Osteogenic activity of the fourteen types of human bone morphogenetic proteins (BMPs). *J. Bone Joint Surg Am. 85* (8), 1544−1552.
(45) Kang, Q., Song, W. X., Luo, Q., et al. (2009) A comprehensive analysis of the dual roles of BMPs in regulating adipogenic and osteogenic differentiation of mesenchymal progenitor cells. *Stem Cells Dev. 18* (4), 545−559.
(46) Kang, Q., Sun, M. H., Cheng, H., et al. (2004) Characterization of the distinct orthotopic bone-forming activity of 14 BMPs using recombinant adenovirus-mediated gene delivery. *Gene Ther. 11* (17), 1312−1320.
(47) Lamplot, J. D., Denduluri, S., Liu, X., Wang, J., Yin, L., Li, R., Shui, W., Zhang, H., Wang, N., Nan, G., et al. (2013) BMP9 signaling in stem cell differentiation and osteogenesis. *Am. J. Stem Cells 2* (1), 1−21.
(48) Luu, H. H., Song, W. X., Luo, X., et al. (2007) Distinct roles of bone morphogenetic proteins in osteogenic differentiation of mesenchymal stem cells. *J. Orthop. Res. 25* (5), 665−677.
(49) Cong, L., Ran, F. A., Cox, D., et al. (2013) Multiplex genome engineering using CRISPR/Cas systems. *Science 339* (6121), 819−823.
(50) Dominguez, A. A., Lim, W. A., and Qi, L. S. (2016) Beyond editing: repurposing CRISPR-Cas9 for precision genome regulation and interrogation. *Nat. Rev. Mol. Cell Biol. 17* (1), 5−15.
(51) Doudna, J. A., and Charpentier, E. (2014) Genome editing. The new frontier of genome engineering with CRISPR-Cas9. *Science 346* (6213), 1258096.
(52) Wang, H., La Russa, M., and Qi, L. S. (2016) CRISPR/Cas9 in Genome Editing and Beyond. *Annu. Rev. Biochem. 85*, 227−264.
(53) Breunig, C. T., Durovic, T., Neuner, A. M., et al. (2018) One step generation of customizable gRNA vectors for multiplex CRISPR approaches through string assembly gRNA cloning (STAgR). *PLoS One 13* (4), e0196015.
(54) Zuckermann, M., Hlevnjak, M., Yazdanparast, H., Zapatka, M., Jones, D. T. W., Lichter, P., and Gronych, J. (2018) A novel cloning strategy for one-step assembly of multiplex CRISPR vectors. *Sci. Rep. 8* (1), 17499.
(55) Wu, N., Zhang, H., Deng, F., et al. (2014) Overexpression of Ad5 precursor terminal protein accelerates recombinant adenovirus packaging and amplification in HEK-293 packaging cells. *Gene Ther. 21* (7), 629−637.
(56) Wei, Q., Fan, J., Liao, J., et al. (2017) Engineering the Rapid Adenovirus Production and Amplification (RAPA) Cell Line to Expedite the Generation of Recombinant Adenoviruses. *Cell. Physiol. Biochem. 41* (6), 2383−2398.
(57) Huang, E., Bi, Y., Jiang, W., et al. (2012) Conditionally immortalized mouse embryonic fibroblasts retain proliferative activity without compromising multipotent differentiation potential. *PLoS One 7* (2), e32428.
(58) Wang, N., Zhang, W., Cui, J., et al. (2014) The piggyBac transposon-mediated expression of SV40 T antigen efficiently immortalizes mouse embryonic fibroblasts (MEFs). *PLoS One 9* (5), e97316.
(59) Zhu, G. H., Huang, J., Bi, Y., et al. (2009) Activation of RXR and RAR signaling promotes myogenic differentiation of myoblastic C2C12 cells. *Differentiation 78* (4), 195−204.
(60) Luo, X., Wang, C.-Z., Chen, J., Song, W.-X., Luo, J., Tang, N., He, B.-C., Kang, Q., Wang, Y., Du, W., et al. (2008) Characterization of gene expression regulated by American ginseng and ginsenoside Rg3 in human colorectal cancer cells. *Int. J. Oncol. 32* (5), 975−983.
(61) Liao, J., Wei, Q., Fan, J., et al. (2017) Characterization of retroviral infectivity and superinfection resistance during retrovirus-mediated transduction of mammalian cells. *Gene Ther. 24* (6), 333−341.
(62) Yu, X., Chen, L., Wu, K., et al. (2018) Establishment and functional characterization of the reversibly immortalized mouse glomerular podocytes (imPODs). *Genes Dis. 5* (2), 137−149.
(63) He, T. C., Zhou, S., da Costa, L. T., Yu, J., Kinzler, K. W., and Vogelstein, B. (1998) A simplified system for generating recombinant adenoviruses. *Proc. Natl. Acad. Sci. U. S. A. 95* (5), 2509−2514.
(64) Luo, J., Deng, Z. L., Luo, X., et al. (2007) A protocol for rapid generation of recombinant adenoviruses using the AdEasy system. *Nat. Protoc. 2* (5), 1236−1247.
(65) Breyer, B., Jiang, W., Cheng, H., et al. (2001) Adenoviral vector-mediated gene transfer for human gene therapy. *Curr. Gene Ther. 1* (2), 149−162.
(66) Lee, C. S., Bishop, E. S., Zhang, R., et al. (2017) Adenovirus-Mediated Gene Delivery: Potential Applications for Gene and Cell-Based Therapies in the New Era of Personalized Medicine. *Genes Dis. 4* (2), 43−63.
(67) Fan, J., Wei, Q., Liao, J., Zou, Y., Song, D., Xiong, D., Ma, C., Hu, X., Qu, X., Chen, L., et al. (2017) Noncanonical Wnt signaling plays an important role in modulating canonical Wnt-regulated stemness, proliferation and terminal differentiation of hepatic progenitors. *Oncotarget. 8* (16), 27105−27119.
(68) Zhao, C., Wu, N., Deng, F., et al. (2014) Adenovirus-mediated gene transfer in mesenchymal stem cells can be significantly enhanced by the cationic polymer Polybrene. *PLoS One 9* (3), e92908.
(69) Wang, N., Zhang, H., Zhang, B. Q., et al. (2014) Adenovirus-mediated efficient gene transfer into cultured three-dimensional organoids. *PLoS One 9* (4), e93608.
(70) Zhao, C., Zeng, Z., Qazvini, N. T., et al. (2018) Thermoresponsive Citrate-Based Graphene Oxide Scaffold Enhances Bone Regeneration from BMP9-Stimulated Adipose-Derived Mesenchymal Stem Cells. *ACS Biomater. Sci. Eng. 4* (8), 2943−2955.
(71) Hu, N., Jiang, D., Huang, E., Liu, X., Li, R., Liang, X., Kim, S. H., Chen, X., Gao, J.-L., Zhang, H., et al. (2013) BMP9-regulated angiogenic signaling plays an important role in the osteogenic

DOI: 10.1021/acssynbio.9b00203
ACS Synth. Biol. 2019, 8, 2092−2105

differentiation of mesenchymal progenitor cells. *J. Cell Sci. 126* (2), 532−541.
(72) Zhao, C., Qazvini, N. T., Sadati, M., et al. (2019) A pH-Triggered, Self-Assembled, and Bioprintable Hybrid Hydrogel Scaffold for Mesenchymal Stem Cell Based Bone Tissue Engineering. *ACS Appl. Mater. Interfaces 11* (9), 8749−8762.
(73) Shu, Y., Yang, C., Ji, X., et al. (2018) Reversibly immortalized human umbilical cord-derived mesenchymal stem cells (UC-MSCs) are responsive to BMP9-induced osteogenic and adipogenic differentiation. *J. Cell. Biochem. 119* (11), 8872−8886.
(74) Zhang, Q., Wang, J., Deng, F., et al. (2015) TqPCR: A Touchdown qPCR Assay with Significantly Improved Detection Sensitivity and Amplification Efficiency of SYBR Green qPCR. *PLoS One 10* (7), e0132666.
(75) Cui, J., Zhang, W., Huang, E., et al. (2019) BMP9-induced osteoblastic differentiation requires functional Notch signaling in mesenchymal stem cells. *Lab. Invest. 99* (1), 58−71.
(76) Feng, T., Li, Z., Jiang, W., et al. (2002) Increased efficiency of cloning large DNA fragments using a lower copy number plasmid. *BioTechniques 32* (5), 992, () 994, 996passim.
(77) Park, J. Y., Luo, Q., Jiang, W., et al. (2004) Dual regulation of gene expression mediated by tetracycline and Cre recombinase. *BioTechniques 36* (3), 390−392, () 394, 396.
(78) Yu, X., Liu, F., Zeng, L., et al. (2018) Niclosamide Exhibits Potent Anticancer Activity and Synergizes with Sorafenib in Human Renal Cell Cancer Cells. *Cell. Physiol. Biochem. 47* (3), 957−971.
(79) Deng, Y., Zhang, J., Wang, Z., Yan, Z., Qiao, M., Ye, J., Wei, Q., Wang, J., Wang, X., Zhao, L., et al. (2015) Antibiotic monensin synergizes with EGFR inhibitors and oxaliplatin to suppress the proliferation of human ovarian cancer cells. *Sci. Rep. 5*, 17523.
(80) Zhao, X.-W., Zhan, Y.-B., Bao, J.-J., Zhou, J.-Q., Zhang, F.-J., Bin, Y., Bai, Y.-H., Wang, Y.-M., Zhang, Z.-Y., and Liu, X.-Z. (2017) Anthelmintic mebendazole enhances cisplatin's effect on suppressing cell proliferation and promotes differentiation of head and neck squamous cell carcinoma (HNSCC). *Oncotarget. 8* (8), 12968−12982.
(81) Wang, X., Wu, X., Zhang, Z., Ma, C., Wu, T., Tang, S., Zeng, Z., Huang, S., Gong, C., Yuan, C., et al. (2018) Monensin inhibits cell proliferation and tumor growth of chemo-resistant pancreatic cancer cells by targeting the EGFR signaling pathway. *Sci. Rep. 8* (1), 17914.
(82) Lu, S., Wang, J., Ye, J., et al. (2016) Bone morphogenetic protein 9 (BMP9) induces effective bone formation from reversibly immortalized multipotent adipose-derived (iMAD) mesenchymal stem cells. *Am. J. Transl Res. 8* (9), 3710−3730.
(83) Ye, J., Wang, J., Zhu, Y., et al. (2016) A thermoresponsive polydiolcitrate-gelatin scaffold and delivery system mediates effective bone formation from BMP9-transduced mesenchymal stem cells. *Biomed Mater. 11* (2), 025021.
(84) Chen, L., Jiang, W., Huang, J., et al. (2010) Insulin-like growth factor 2 (IGF-2) potentiates BMP-9-induced osteogenic differentiation and bone formation. *J. Bone Miner. Res. 25* (11), 2447−2459.
(85) Liao, Z., Nan, G., Yan, Z., et al. (2015) The Anthelmintic Drug Niclosamide Inhibits the Proliferative Activity of Human Osteosarcoma Cells by Targeting Multiple Signal Pathways. *Curr. Cancer Drug Targets 15* (8), 726−738.
(86) Li, R., Zhang, W., Cui, J., et al. (2014) Targeting BMP9-promoted human osteosarcoma growth by inactivation of notch signaling. *Curr. Cancer Drug Targets 14* (3), 274−285.
(87) Zou, Y., Qazvini, N. T., Zane, K., et al. (2017) Gelatin-Derived Graphene-Silicate Hybrid Materials Are Biocompatible and Synergistically Promote BMP9-Induced Osteogenic Differentiation of Mesenchymal Stem Cells. *ACS Appl. Mater. Interfaces 9* (19), 15922−15932.
(88) Zhang, J., Weng, Y., Liu, X., et al. (2013) Endoplasmic reticulum (ER) stress inducible factor cysteine-rich with EGF-like domains 2 (Creld2) is an important mediator of BMP9-regulated osteogenic differentiation of mesenchymal stem cells. *PLoS One 8* (9), e73086.
(89) Huang, E., Zhu, G., Jiang, W., et al. (2012) Growth hormone synergizes with BMP9 in osteogenic differentiation by activating the JAK/STAT/IGF1 pathway in murine multilineage cells. *J. Bone Miner. Res. 27* (7), 1566−1575.

DOI: 10.1021/acssynbio.9b00203
ACS Synth. Biol. 2019, 8, 2092−2105